Controlling Conformational Flexibility of an O_2-Binding H-NOX Domain

Emily E. Weinert, Christine M. Phillips-Piro, Rosalie Tran, Richard A. Mathies, Michael A. Marletta

Supporting Information

Figure S1. Comparison of the heme pockets of *Tt* H-NOX (shown in teal; PDB ID 1U55 (*1*)) and sperm whale myoglobin (shown in purple; PDB ID 1A6M (*2*)). Key residues in the pocket are shown in orange sticks with nitrogens in blue and oxygens in red. Hydrogen bonding interactions between the protein and the bound oxygen molecule are shown in dashed black lines.

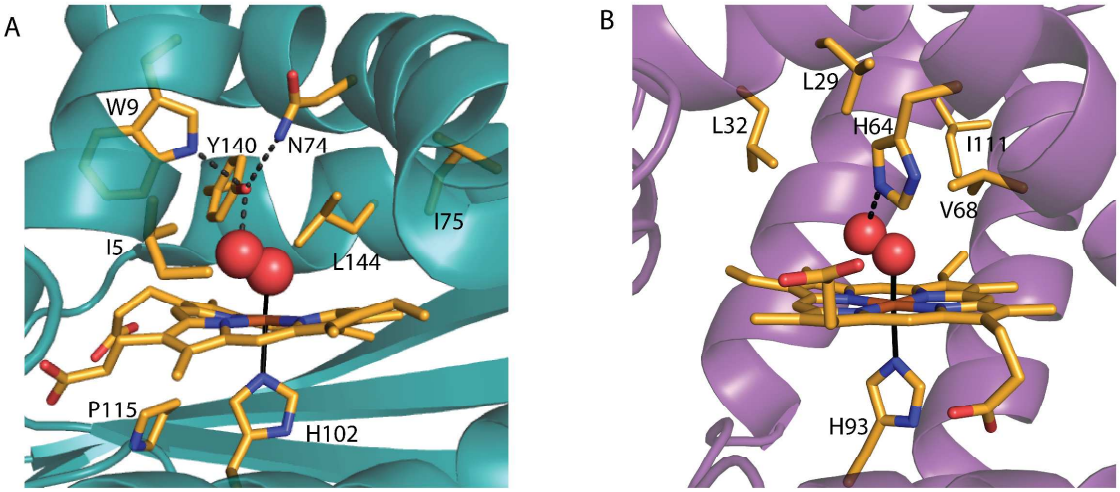

Figure S2. Resonance Raman spectra of WT, I5F, I75F, and L144F *Tt* H-NOX. The I5F mutant exhibits the most peak broadening and heme flexibility of all the mutants.

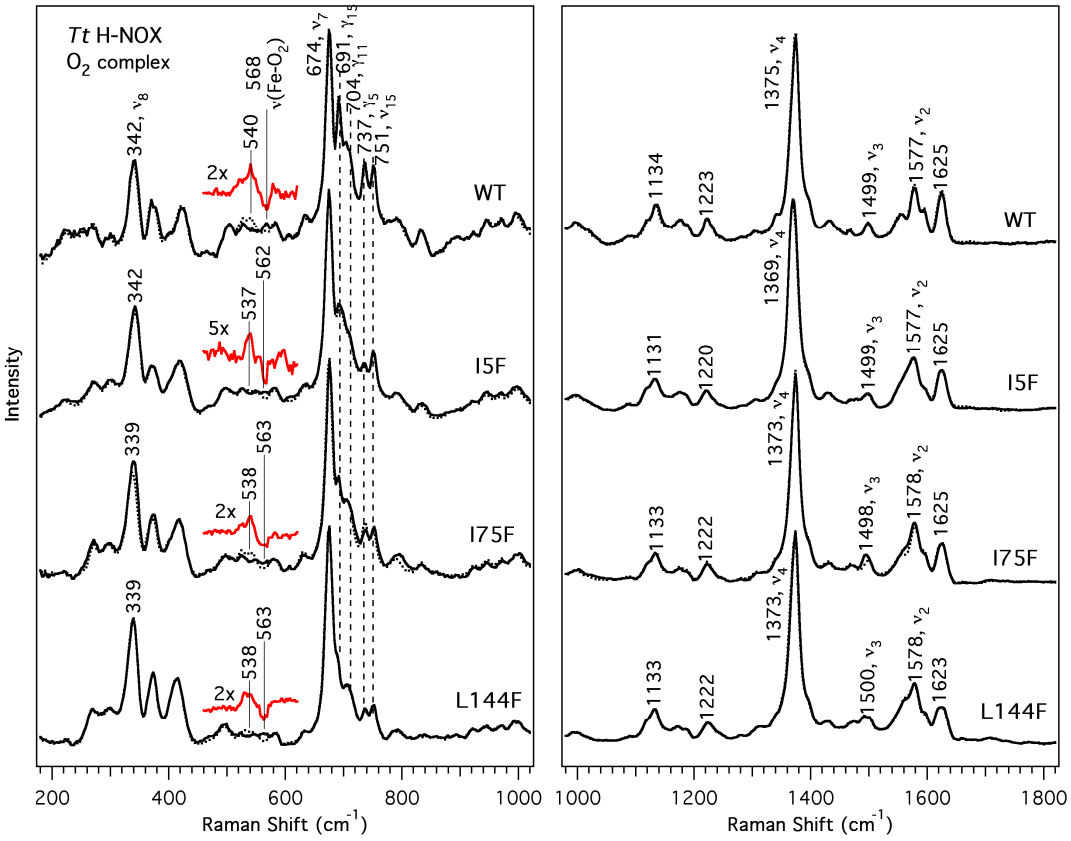

Figure S3. Composite omit map density of the disordered loop, residues 27-47, in the I5F *Tt* H-NOX structure. (A) To orient the loop with residues in the loop as well as H102 and the heme shown in stick. (B) Zoom-in of the loop region (boxed on right in (A)) with only the loop and heme shown for clarity. Electron density is contoured at 1.0 σ and is shown for the heme cofactor for comparison.

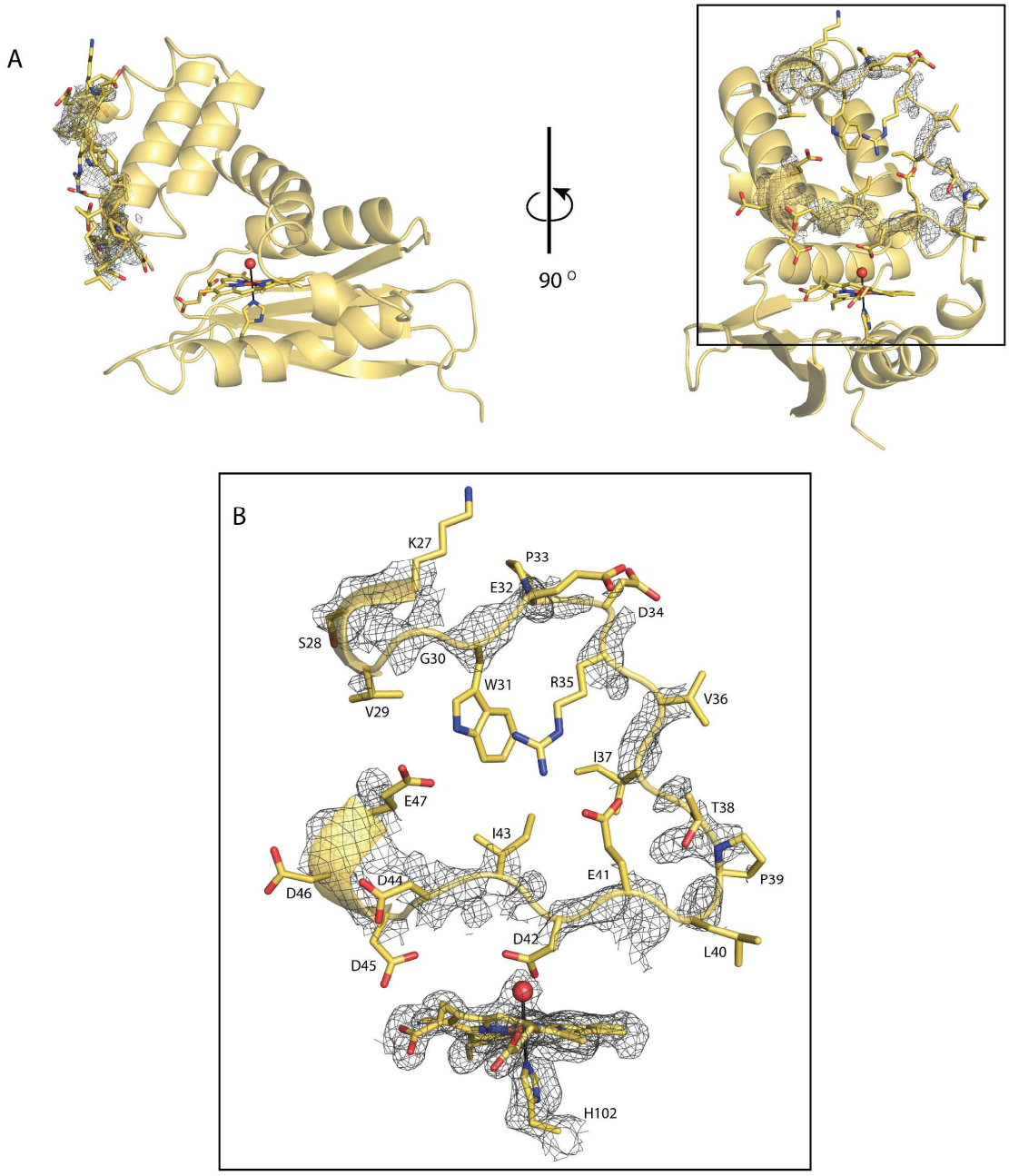

Figure S4. Residues F5 and F78 in the heme pocket are present in two distinct side chain conformations. A composite omit map contoured at 1.0 σ is shown in grey mesh. The two conformations of the first N-terminal amino acids and F78 are shown in stick as well as the heme and H102. Density for the heme, water, and H102 are shown for comparison.

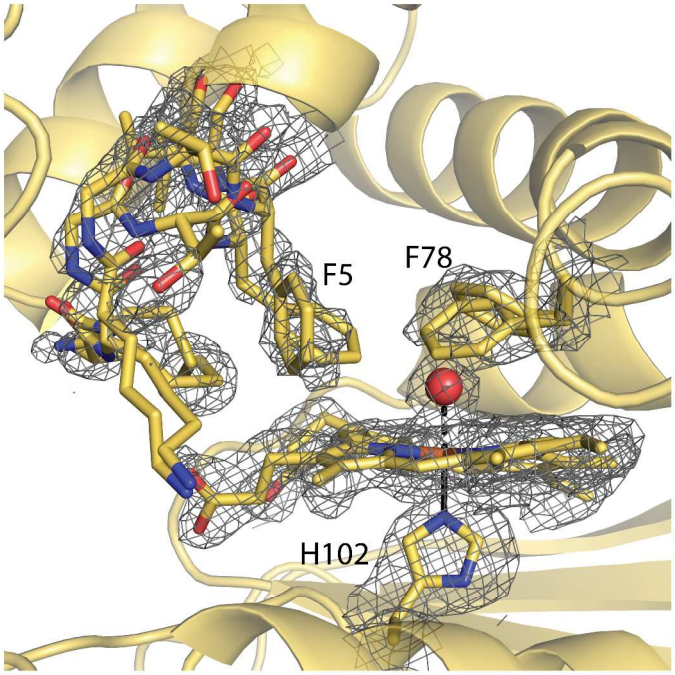

Table S1: Electronic absorption data.

Protein	Soret	β	α	Ref.
Unligated				
WT	431	568		(*3*)
I5F	432	563		this work
I5F/I75F	432	563		this work
I5F/L144F	432	555		this work
I5F/I75F/L144F	432	556		this work
O_2 bound				
WT	416	556	591	(*3*)
I5F	417	552	590	this work
I5F/I75F	418	551	585	this work
I5F/L144F	419	547	580	this work
I5F/I75F/L144F	421	546	578	this work
CO bound				
WT	424	544	565	(*3*)
I5F	425	546	569	this work
I5F/I75F	425	548	571	this work
I5F/L144F	424	544	571	this work
I5F/I75F/L144F	424	544	572	this work
NO bound				
WT	420	547	575	(*3*)
I5F	421, 399sh	551	578	this work
I5F/I75F	403, 417	552	578	this work
I5F/L144F	422, 403	551	578	this work
I5F/I75F/L144F	422, 404	552	578	this work

Table S2. NO dissociation rates.[a]

Tt H-NOX	$k_{off,fast}$ NO ($x10^{-4}$ s^{-1})	$k_{off,slow}$ NO ($x10^{-4}$ s^{-1})	Fe-NO Coord	Ref.
WT	6.29 ± 0.48	1.31 ± 0.22	6	*(3)*
I75F	15.68 ± 2.87	4.15 ± 0.78	5/6	*(4),* this work
L144F	1.85 ± 0.85	1.08 ± 0.33	5/6	*(4),* this work
I75F/L144F	4.52 ± 0.87	1.28 ± 0.04	5/6	*(4),* this work
I5L	8.93 ± 0.82	3.99 ± 0.58	6	this work
I5F	[b]	1.10 ± 0.16	6	this work
I5F/I75F	1.39 ± 0.37	0.465 ± 0.0503	5/6	this work
I5F/L144F	1.75 ± 0.017	0.398 ± 0.081	5/6	this work
I5F/I75F/L144F	1.94 ± 0.11	0.517 ± 0.037	5/6	this work

[a] NO dissociation rate measurement**.** NO dissociation rates were performed as previously described (*4, 5*). Briefly, Fe^{II}-NO complexes were rapidly mixed with equivolume of buffer B containing saturated CO and 30 mM dithionite (final concentration) as an NO trap. Data were acquired on either a Cary 3E spectrophotomer equipped with a Neslab RTE-100 constant temperature bath or a Cary 300Bio with Peltier accessory with the temperature bath set to 20 °C. The NO dissociation rate was determined from the increase in the maximum of the Fe(II)-CO spectra over time.

[b] The biexponential NO dissociation rates for the mutants that are a mixute of 5/6 coordinate Fe^{II}-NO are likely due to the required conversion from 5 to 6 coordinate to allow NO dissociation. In addition, the biexponential behavior may also be due to interconversion of multiple protein conformations in solution (*6*). *Tt* WT and I5L proteins exhibit biexponential behavior despite the Fe^{II}-NO adduct being solely 6 coordinate. This is likely due to multiple protein conformations in solution that alter the rates of NO dissociation. In contrast, the NO dissociation rate for the I5F mutant is monoexponential. This is likely due to the increased flexibility leading to rapid interconversion of the various solution conformations of the protein.

Table S3: Resonance Raman skeletal markers.

Protein	Ligand	ν_{10}	ν_2	ν_3	ν_4	ν(Fe-O_2)	Ref.
Tt WT	O_2	1624	1579	1499	1375	567	(*3, 7*)
Tt I5L	O_2	1627	1580	1499	1372	564	(*7*)
Tt I5F	O_2	1625	1577	1499	1369	562	this work

1. Pellicena, P., Karow, D. S., Boon, E. M., Marletta, M. A., and Kuriyan, J. (2004) Crystal structure of an oxygen-binding heme domain related to soluble guanylate cyclases, *Proc Natl Acad Sci USA 101*, 12854-12859.
2. Vojtechovsky, J., Chu, K., Berendzen, J., Sweet, R. M., and Schlichting, I. (1999) Crystal structures of myoglobin-ligand complexes at near-atomic resolution, *Biophys J 77*, 2153-2174.
3. Karow, D. S., Pan, D., Tran, R., Pellicena, P., Presley, A., Mathies, R. A., and Marletta, M. A. (2004) Spectroscopic characterization of the soluble guanylate cyclase-like heme domains from *Vibrio cholerae* and *Thermoanaerobacter tengcongensis*, *Biochemistry 43*, 10203-10211.
4. Weinert, E. E., Plate, L., Whited, C. A., Olea, C., Jr., and Marletta, M. A. (2010) Determinants of ligand affinity and heme reactivity in H-NOX domains, *Angew Chem Int Ed Engl 49*, 720-723.
5. Boon, E. M., Huang, S. H., and Marletta, M. A. (2005) A molecular basis for NO selectivity in soluble guanylate cyclase, *Nature Chem Biol 1*, 53-59.
6. Boon, E. M., Davis, J. H., Tran, R., Karow, D. S., Huang, S. H., Pan, D., Miazgowicz, M. M., Mathies, R. A., and Marletta, M. A. (2006) Nitric oxide binding to prokaryotic homologs of the soluble guanylate cyclase beta1 H-NOX domain, *J Biol Chem 281*, 21892-21902.
7. Tran, R., Boon, E. M., Marletta, M. A., and Mathies, R. A. (2009) Resonance Raman spectra of an O_2-binding H-NOX domain reveal heme relaxation upon mutation, *Biochemistry 48*, 8568-8577.